Immuno-electron cryo-microscopy imaging reveals a looped topology of apoB at the surface of human LDL ⓢ

Yuhang Liu and David Atkinson[1]

Department of Physiology and Biophysics, Boston University School of Medicine, Boston, MA 02118

Abstract   A single copy of apoB is the sole protein component of human LDL. ApoB is crucial for LDL particle stabilization and is the ligand for LDL receptor, through which cholesterol is delivered to cells. Dysregulation of the pathways of LDL metabolism is well documented in the pathophysiology of atherosclerosis. However, an understanding of the structure of LDL and apoB underlying these biological processes remains limited. In this study, we derived a 22 Å-resolution three-dimensional (3D) density map of LDL using cryo-electron microscopy and image reconstruction, which showed a backbone of high-density regions that encircle the LDL particle. Additional high-density belts complemented this backbone high density to enclose the edge of the LDL particle. Image reconstructions of monoclonal antibody-labeled LDL located six epitopes in five putative domains of apoB in 3D. Epitopes in the LDL receptor binding domain were located on one side of the LDL particle, and epitopes in the N-terminal and C-terminal domains of apoB were in close proximity at the front side of the particle. Such image information revealed a looped topology of apoB on the LDL surface and demonstrated the active role of apoB in maintaining the shape of the LDL particle.—Liu, Y., and D. Atkinson. **Immuno-electron cryo-microscopy imaging reveals a looped topology of apoB at the surface of human LDL.** *J. Lipid Res.* **2011.** 52: 1111–1116.

Supplementary key words   low-density lipoprotein structure • apolipoprotein B structure • apolipoprotein B epitope location • proteoglycan binding • cholesterol transport

ApoB is the sole protein content of human LDL, which serves as a primary mechanism to transport cholesterol from the liver to the peripheral tissue through the circulation. LDL is derived from VLDL through the VLDL-LDL pathway (1). These lipoprotein particles have a neutral lipid core that cannot exist in a stable state in the hydrophilic environment of the blood. Thus, apoB is absolutely required for the initial assembly of the VLDL particle and associates with lipoprotein particles as a nonexchangeable apolipoprotein that is responsible for the stabilization of the particles (2, 3). On the LDL particle surface, apoB is the ligand for the LDL receptor. For LDL that undergoes prolonged retention in the arterial intima, the apoB moiety on LDL is also involved in interactions with proteoglycans in the early events of arteriosclerosis (4–6). Thus, apoB plays an important role in lipid metabolism, and structural information on the organization of the LDL particle is key to understanding the details of the interactions of the apoB-containing particles with other proteins and receptors in both physiological and pathophysiological conditions. However, with 4,536 amino acids and properties designed for association with the lipids, apoB presents a challenge for structural studies. Currently, no high-resolution image information of any domain of apoB is available from experimental studies. Analysis of the primary sequence suggests that apoB contains amphipathic α-helix and β-sheet secondary structures with different lipid binding affinities. ApoB can be divided into five putative domains that are enriched with these amphipathic secondary structural elements in a proposed five-domain model of apoB (1, 7). Chatterton et al. (8, 9) pioneered studies to determine the distribution of apoB on the surface of LDL by employing the strategy of using paired monoclonal antibody (MAb) labeling to obtain projection images with negative stain electron microscopy followed by triangulation to determine the corresponding MAb locations. However, later work from several cryo-electron microscopy (cryo-EM) groups has shown that LDL is a discoidal-shaped particle at a temperature below the phase transition associated with the core-located cholesteryl esters (10–13). Thus, the underlying assumption that LDL is a spherical particle limits the accuracy of the triangulation measurements. More importantly, the handedness of the antibody-LDL complex cannot be determined from the projection images alone, and thus, the relative positions of

the antibodies based on triangulation may be in mirror symmetry-related locations.

In comparison to studies based on other methodologies (8, 9, 14, 15), cryo-EM and image reconstruction have more advantages in preserving the LDL particle in the native state, and intuitively reveal the density distribution of the LDL structure in three-dimensional (3D) images (10–12, 16). Previously, we have shown, in the 3D density map, that the apoB protein component corresponds to the high-density regions and distributes on the edge of the particle (16). In this study, we derived a higher resolution 3D structure of LDL that better resolved the high-density features and revealed the distribution of apoB in more detail. Furthermore, we performed image reconstructions of MAb-labeled LDL. The common structural features from the MAb-labeled LDL enabled us to resolve the relative handedness and locate the epitope positions that encompass apoB in five putative domains, including the LDL receptor binding domain, and the N terminus and C terminus of apoB. Together, this image information provides new insights into the apoB stabilization of the LDL particle, and suggests a destabilizing effect on LDL structure that may happen through the interaction of apoB and proteoglycans.

MATERIALS AND METHODS

LDL preparation and characterization

A highly homogeneous subfraction of LDL with a narrow buoyant density range (1.035–1.04 mg/ml) was obtained by three rounds of KBr density gradient ultracentrifugation and characterized as described previously (10, 16).

Monoclonal antibody labeling

The Mb3, Mb11, and Mb19 antibodies were acquired as gifts from the laboratory of Dr. Linda Curtiss (The Scripps Research Institute, La Jolla, CA), and Bsol4, Bsol7, and 5E11 antibodies were obtained as gifts from Dr. Yves Marcel and Dr. Ross W. Milne (University of Ottawa, Ottawa, ON, Canada). The antibodies were received in the form of mouse ascites. The IgG proteins were purified from ascites using an ImmunoPure® plus immobilized protein A IgG purification kit. The purified MAbs were divided into aliquots and stored at −80°C until use. For MAb labeling of LDL, equal molar quantities of the MAb and apoB (0.1 mg/ml apoB) were mixed well and allowed to react for 3 h at ambient temperature before use for cryo-plunging preservation.

Sample cryo-preservation

The LDL- and MAb-labeled LDL samples were cryo-preserved using the Vitrobot® system as described previously (10, 16). The samples were incubated in the chamber at 22°C and 100% humidity.

Cryo-EM and image processing

Images were collected on a Tecnai TF20 electron microscope with an Oxford® cryo-holder using low-dose conditions. The data sets for LDL, LDL+Bsol4, and LDL+Mb11 samples were collected with 50,000× magnification and recorded on KODAK SO163 film. The films were digitized with a Creo EVERSMART® scanner and binned on a Linux computer. After binning, the image file was 2.73 Å/pixel. The data for LDL+Mb3, LDL+Mb19,

LDL+5E11, and LDL+Bsol7 samples were collected with 29,000× magnification and recorded on a 4K TVIPS® CCD camera. The image file was at 2.9 Å/pixel.

For image reconstruction, particle images were picked with *e2boxer* from the EMAN2 program package (17) and contrast transfer function (CTF) correction was performed with *ctfit* from the EMAN program package. The CTF-corrected images were further binned twice before structure reconstruction with the EMAN program (18). The numbers of particles contained in the data sets were LDL (∼21,000), Mb19-labeled (∼14,000), Mb3-labeled (∼11,000), Mb11-labeled (∼17,500), Bsol4-labeled (∼9,200), 5E11-labeled (∼14,000), and Bsol7-labeled (∼10,000). The resolutions of the reconstructions were determined with Fourier Shell Correlation at a cutoff of 0.5 (see supplementary Fig. I).

The image reconstruction image results were displayed with the EMAN and Chimera program packages (19).

RESULTS AND DISCUSSION

Overall distribution of apoB

The structure map of LDL revealing the high density distributed at the surface of LDL is shown in **Fig. 1** and supplementary movie 2. The structure exhibited the same overall shape and the protrusion in the pointed end as described previously (16). The high-density regions are better resolved and can be dissected into three regions based on continuity and the location at the LDL particle surface. A backbone of a high-density belt, which is colored in gold, runs around the particle surface. The belt runs along the upper rim of the right side of the particle and lower rim of the left side and crosses over at the front and back sides of the particle to form an enclosed circle. The second group of high-density regions (green) contours the rims of the discoidal-shaped particle and complements the backbone to form a circle on the edge of the two flat surfaces. In this way, the two flat surface regions with generally somewhat lower-density areas are enclosed. The third regions (yellow) are the densities on the side wall of the LDL particle that emanate from the backbone. On the right side of the LDL particle, these high-density regions run parallel to the flat surfaces of the LDL particle
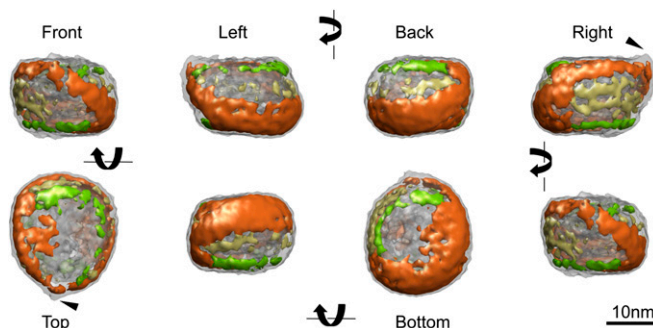

Fig. 1. High-density distribution of the LDL particle. The larger volume in gray represents the overall shape of the LDL particle, which is overlaid with the high-density regions that are color-coded as described in the text. The overlaid structure was turned 90° in each frame and displayed from right to left in the first row and from left to right in the second row. The position of the protrusion is indicated by triangles in the *right* and *top* views.

and the layered cholesteryl ester core that exists at a temperature below the lipid core thermal phase transition (10). Our previous studies have shown that the high-density regions in the LDL structural volumes arise from the protein component and the lower density regions on the flat surfaces are mainly from the monolayer of phospholipids (16). Thus, the high-density regions shown in this 22 Å-resolution density map reflect the distribution of apoB at the surface of the LDL particle. The structure confirms our previous conclusion that the flat surfaces are mainly covered by the monolayer of phospholipid and, further, shows that the two flat surfaces of the monolayer of phospholipids are enclosed by a high-density circle of protein around the edge and are confined in a two-dimensional array. Furthermore, apoB forms a closed circle around the edge of the discoidal-shaped LDL particle, which suggests that rather than "floating" on the lipid droplet, apoB forms a defined loop structure. Thus, the looped apoB may accommodate variable numbers of lipid molecules, which results in different particle sizes, by the expulsion of exchangeable regions of apoB from the surface, rearrangement of domains, or adjustment of the curvature of the

loop during the VLDL-IDL-LDL and LDL subspecies transitions (14, 20, 21).

Antibody labeling to determine the epitope positions in 3D

To interpret further the structure volume with additional experimental constraints, we used monoclonal antibodies to label the apoB on LDL, followed by 3D image reconstruction to reveal the corresponding apoB epitope positions at the surface in 3D. We labeled LDL with six monoclonal antibodies individually, and used the same image reconstruction procedures. Image results from the six MAb-labeled LDLs are shown in **Fig. 2**.

Taking the MAb (5E11)-labeled LDL as an example, the projection images showed the LDL particle with the same intrinsic pointed feature of LDL (indicated by the triangle) as reported previously (16). In addition, a dark density region on the surface of the LDL particle from the bound IgG protein (indicated by the arrow) was clearly observed. The IgG molecule is an ∼150 kDa protein and is flexible in shape (22). Thus, one of the Fab regions of IgG that bound to the LDL particle will be more fixed relative to the LDL particle, and the remaining part of the IgG
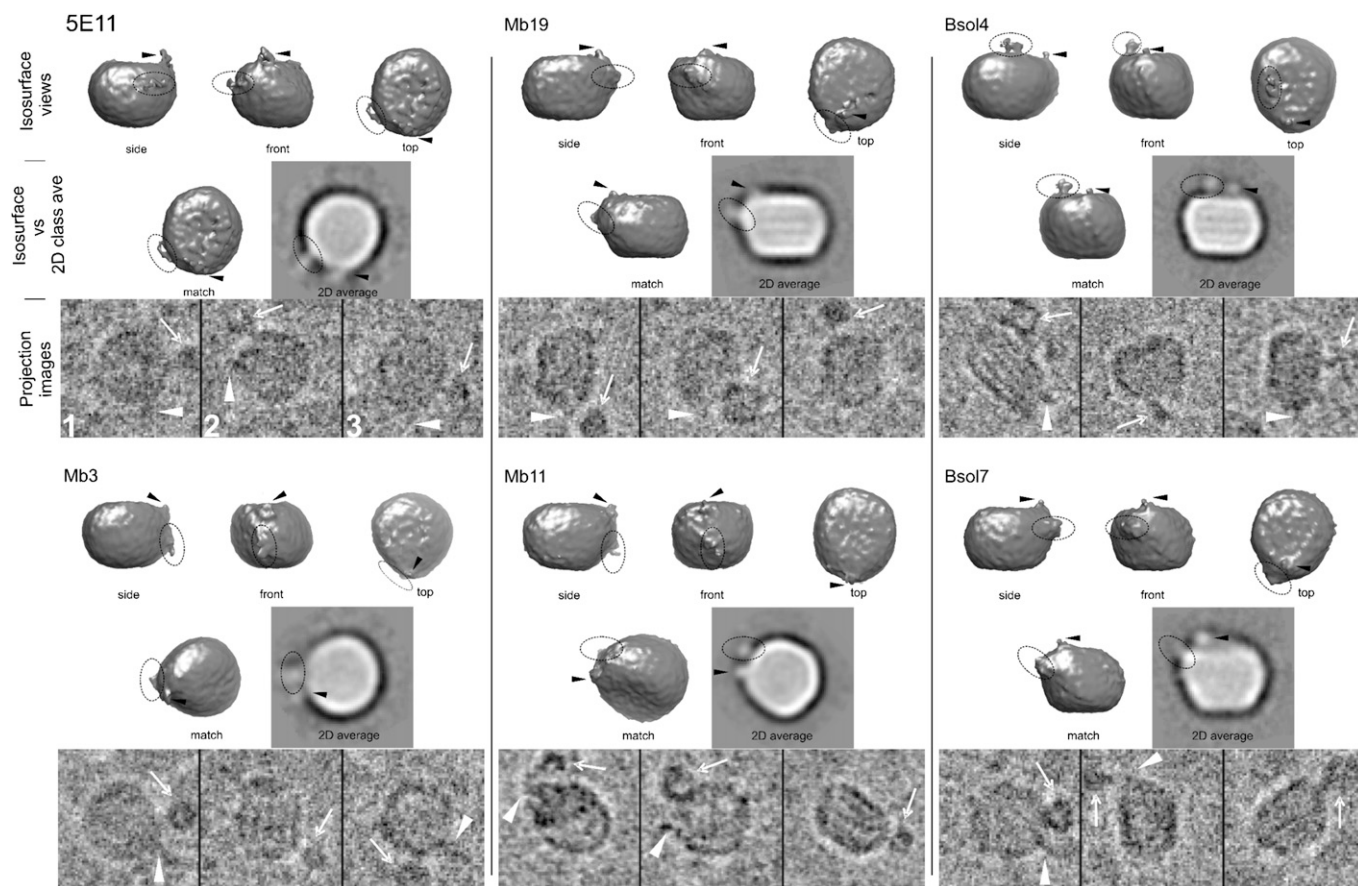

Fig. 2. Locating MAbs on the surface of the LDL particle. The results of each MAb (5E11, Mb19, Mb3, Mb11, Bsol4, and Bsol7)-labeled LDL are displayed in the same way. For each MAb, three 2D projection images are shown at the bottom; the dark regions are electron dense. The positions of the pointed feature and the bound IgG protein are indicated by a triangle and arrow, respectively. The structure volume of the MAb and LDL complex is shown in the three views at the top. The iso-surface display of the 3D structure is positioned in a matching orientation to compare with the 2D class average image for the positions of the bound MAb and the protruding densities that correspond to the pointed feature of LDL, respectively. In the 3D reconstruction and 2D class average images, the protrusion from the LDL intrinsic pointed feature is indicated by the triangle and the location of the extra density corresponding to the MAb is circled. The 5E11-labeled LDL was explained in the text as an example and the 2D projection images are numbered.

protein will exhibit more flexibility. As expected, taking the LDL particle center as the rotation center, the angles between the pointed feature and the IgG protein varied in the three images because of the different orientations of the particles and the flexibility of both of these surface features. The classification of the 2D projection images similarly showed a class average image with two density regions extruding from the circularly shaped LDL particle projection image that can be attributed to the pointed feature of the LDL and to the bound IgG protein.

In the 3D image reconstruction, the MAb (5E11)-labeled LDL particle exhibited the same structural features as unlabeled LDL in terms of the particle shape and the intrinsic protruding density at the LDL surface. In addition, an extra density in the 5E11-labeled reconstruction was apparent at the surface of the LDL particle. As expected for the flexibility of the IgG protein, this extra density was only seen clearly above the background in immediate proximity to the LDL particle and became less distinctive in the region further away from the particle surface. Following the adjustment of the orientation of the 3D structure volume, the shape of the LDL-IgG complex and the relative position of the protrusion and the extra density were similar to the result from the class average images. This suggests that the extra density seen in both the 3D structure volume and the class average image were from the antibody labeling.

It is important to note that for 5E11-labeled LDL, the second projection image exhibited an opposite handedness compared with the first and the third images. The absolute handedness of the LDL particle could not be determined from the projection images alone or from the reconstruction of these untilted projection images. Thus, we aligned the 3D volumes of the six independent reconstructions and assigned the relative handedness based on the high-density backbone and the intrinsic protrusion of the LDL particle that served as common morphological features.

Positions of apoB functional domains

The primary sequence locations of the epitopes of the MAb used in the labeling are color coded in **Fig. 3A**. These epitopes are located in the five putative domains of apoB (1, 23). The 3D locations of the MAbs to these epitopes are shown in Fig. 3B and supplementary movie 3. Mb19 (colored in blue) labels the N-terminal region of apoB [residue ~70 (24)] and was found below the "pointed feature" on the front side. Thus, this position corresponds to the starting point of apoB. The Mb11 and Mb3 (colored in violet) have their epitopes roughly in the same range in the apoB sequence [residues 1,022–1,031 (23)], which is at the beginning of the second putative domain. In the 3D images, the two antibodies were found at a similar location, which was in the lower part of the front side. The position of Bsol4 [colored in light blue, residues ~2,488–2,543 (23)] was found on the upper edge of the flat surface on the right of the particle, where the backbone density circled the LDL particle about 3/4 turn. The MAb 5E11 [colored in red, residues ~3,441–3,569 (23)] was found on the side wall density on the right side of the par-

ticle and was close to the position of Bsol4. Finally, the Bsol7 MAb [colored in dark green, residues ~4,521–4,536 (23)] was found in the front side at a position close to Mb19. The observation that the MAbs (Mb19, Bsol4, Bsol7, 5E11) were found along the high-density regions of the LDL particle further substantiates that the high-density regions represent the distribution of the apoB protein component as opposed to the phospholipid head groups. The Mb3 and Mb11 MAbs were found at a similar location, which also validates the 3D positions determined from the independent image reconstructions.

The apoB protein starts from its N terminus at the position of Mb19, and the first putative domain ends approximately at residue 1,000, which is close to the epitopes of Mb11 and Mb3. The positions of these two epitopes of apoB were on the front side of the particle, suggesting that the first domain is compact. This observation is in agreement with the overall dimensions of the predicted structure from this domain of apoB (25). The position of 5E11 was found on the right side of the LDL particle on the parallel density regions that emanated from the backbone of apoB. The MAb 5E11 has been shown to block the binding of LDL to the LDL receptor, and the epitope for 5E11 corresponds to the LDL receptor binding site (26, 27). Previous studies have determined that the Mb47 antibody bound to a location similar to that of 5E11 shown here, which is in agreement with the overlapping epitopes for these two MAbs [for details see (28)].

Using a similar approach, Ren et al. (12) observed a high-density protrusion at one end of the long axis of the LDL particle in images of LDL labeled with the LDL receptor extra-cellular domain and proposed that this feature represented the β-propeller domain of the LDL receptor. A distribution of apoB was further proposed
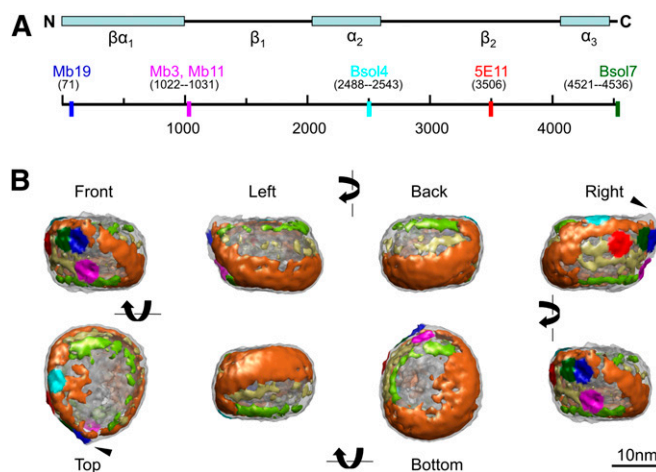

Fig. 3. MAb locations in the primary sequence and on the surface of LDL particle. A: The linear representation of apoB domains with amphipathic α-helix or β-sheet-enriched secondary structures is shown. The epitope positions of the MAbs along the apoB are color-coded, and the epitope residue numbers are indicated. B: The MAb positions with respect to the high-density regions on the surface of the LDL particle. The triangle indicates the position of the intrinsic protrusion of the LDL particle. The locations of MAbs are color coded in the same way as in A.

based on this receptor binding site and the distribution of the high-density regions (12). However, our studies of both MAb-labeled and unlabeled LDL (16) clearly showed an intrinsic pointed feature of LDL at a similar location, which may account for the extra density interpreted as the bound β-propeller domain of the LDL receptor. Furthermore, the epitope location for 5E11 (and for Mb47) determined from this study suggests an alternative LDL receptor binding site on the side rather than on the end of the long axis of the LDL particle. The LDL receptor binding site only forms or becomes exposed after the particle transition from VLDL-IDL to LDL. Thus, the protein structure in this region may be formed by a rearrangement of apoB during the VLDL-LDL transition or may be involved in binding to other proteins that mask this region for LDL receptor binding.

The epitope for Bsol7 represents the position of the C terminus of apoB, and was found on the front side of the LDL particle in close proximity to the epitope position of Mb19. This observation suggests that the ends of the N terminus and C terminus of apoB are close in space and thus may interact with each other to form a closed loop to stabilize the LDL particle.

Because 5E11 and Mb47 share the same epitope, the directly comparable MAb pair results in the studies from Chatterton et al. (9) are Mb19-Mb11, Mb19-Mb47, and Mb11-Mb47. The angles between these paired MAb locations determined from our reconstructions are well matched with the available paired MAb-labeled LDL projection images from the early studies.

Intrinsic protrusion region of apoB

Studies have demonstrated that the first ∼1,000 residues of apoB represent the single largest trypsin-releasable region of apoB (29). This trypsin releasability suggests that this part of apoB is accessible to the aqueous solution and is not in strong association with the bulk of the lipid core. It has also been shown that the first 5.9% of apoB does not process lipid association properties comparable to those seen with the first 17% of apoB (25). Furthermore, the first ∼250 residues of apoB have available proteoglycan binding sites, which can be steric blocked by the binding of the Mb19 monoclonal antibody (5, 6, 27). In our studies, a protrusion at the surface of LDL was found consistently in our 3D image reconstructions. This protrusion exhibited a flexible nature and was the only region at the LDL particle surface that was not associated with the bulk of the particle. This protrusion was close to the epitope of Mb19 in space and stemmed from the front face of the LDL particle, where the first putative domain was located. Together, these observations suggest that this protrusion is part of the N-terminal globular domain of apoB and is possibly the first ∼5.9% nonlipid-associated part of apoB. It has been suggested that the carboxyl terminal domain of apoB-100 can mask the proteoglycan binding site B-Ib (residues 84–94) (5); however, temporary exposure of the B-Ib and other potential proteoglycan binding sites in the N terminus of apoB may possibly be due to the flexible nature of this region. Thus, the proteoglycan binding to this region may disrupt the interaction between the N ter-

minus and the C terminus of apoB. Subsequently, the LDL particle may become unstable and the hydrophobic core may be exposed, resulting in an irreversible structural change preceding the atherosclerosis event, which has been suggested by kinetic X-ray scattering and thermal stability studies (30, 31).⬛

REFERENCES

1. Segrest, J. P., M. K. Jones, H. De Loof, and N. Dashti. 2001. Structure of apolipoprotein B-100 in low density lipoproteins. *J. Lipid Res.* **42:** 1346–1367.
2. Jiang, Z. G., Y. Liu, M. M. Hussain, D. Atkinson, and C. J. McKnight. 2008. Reconstituting initial events during the assembly of apolipoprotein B-containing lipoproteins in a cell-free system. *J. Mol. Biol.* **383:** 1181–1194.
3. Small, D. M., L. Wang, and M. A. Mitsche. 2009. The adsorption of biological peptides and proteins at the oil/water interface. A potentially important but largely unexplored field. *J. Lipid Res.* **50 (Suppl.):** 329–334.
4. Hevonoja, T., M. O. Pentikainen, M. T. Hyvonen, P. T. Kovanen, and M. Ala-Korpela. 2000. Structure of low density lipoprotein (LDL) particles: basis for understanding molecular changes in modified LDL. *Biochim. Biophys. Acta.* **1488:** 189–210.
5. Flood, C., M. Gustafsson, P. E. Richardson, S. C. Harvey, J. P. Segrest, and J. Boren. 2002. Identification of the proteoglycan binding site in apolipoprotein B48. *J. Biol. Chem.* **277:** 32228–32233.
6. Goldberg, I. J., W. D. Wagner, L. Pang, L. Paka, L. K. Curtiss, J. A. DeLozier, G. S. Shelness, C. S. Young, and S. Pillarisetti. 1998. The NH2-terminal region of apolipoprotein B is sufficient for lipoprotein association with glycosaminoglycans. *J. Biol. Chem.* **273:** 35355–35361.
7. Cladaras, C., M. Hadzopoulou-Cladaras, R. T. Nolte, D. Atkinson, and V. I. Zannis. 1986. The complete sequence and structural analysis of human apolipoprotein B-100: relationship between apoB-100 and apoB-48 forms. *EMBO J.* **5:** 3495–3507.
8. Chatterton, J. E., M. L. Phillips, L. K. Curtiss, R. Milne, J. C. Fruchart, and V. N. Schumaker. 1995. Immunoelectron microscopy of low density lipoproteins yields a ribbon and bow model for the conformation of apolipoprotein B on the lipoprotein surface. *J. Lipid Res.* **36:** 2027–2037.
9. Chatterton, J. E., M. L. Phillips, L. K. Curtiss, R. W. Milne, Y. L. Marcel, and V. N. Schumaker. 1991. Mapping apolipoprotein B on the low density lipoprotein surface by immunoelectron microscopy. *J. Biol. Chem.* **266:** 5955–5962.
10. Liu, Y., D. Luo, and D. Atkinson. 2011. Human LDL core cholesterol ester packing: three-dimensional image reconstruction and SAXS simulation studies. *J. Lipid Res.* **52:** 256–262.
11. Orlova, E. V., M. B. Sherman, W. Chiu, H. Mowri, L. C. Smith, and A. M. Gotto, Jr. 1999. Three-dimensional structure of low density lipoproteins by electron cryomicroscopy. *Proc. Natl. Acad. Sci. USA.* **96:** 8420–8425.
12. Ren, G., G. Rudenko, S. J. Ludtke, J. Deisenhofer, W. Chiu, and H. J. Pownall. 2010. Model of human low-density lipoprotein and bound receptor based on cryoEM. *Proc. Natl. Acad. Sci. USA.* **107:** 1059–1064.
13. van Antwerpen, R. 2004. Preferred orientations of LDL in vitreous ice indicate a discoid shape of the lipoprotein particle. *Arch. Biochem. Biophys.* **432:** 122–127.
14. Johs, A., M. Hammel, I. Waldner, R. P. May, P. Laggner, and R. Prassl. 2006. Modular structure of solubilized human apolipoprotein B-100. Low resolution model revealed by small angle neutron scattering. *J. Biol. Chem.* **281:** 19732–19739.
15. Krisko, A., and C. Etchebest. 2007. Theoretical model of human apolipoprotein B100 tertiary structure. *Proteins.* **66:** 342–358.
16. Liu, Y., and D. Atkinson. 2011. Enhancing the contrast of ApoB to locate the surface components in the 3D density map of human LDL. *J. Mol. Biol.* **405:** 274–283.

17. Tang, G., L. Peng, P. R. Baldwin, D. S. Mann, W. Jiang, I. Rees, and S. J. Ludtke. 2007. EMAN2: an extensible image processing suite for electron microscopy. *J. Struct. Biol.* **157:** 38–46.

18. Ludtke, S. J., P. R. Baldwin, and W. Chiu. 1999. EMAN: semiautomated software for high-resolution single-particle reconstructions. *J. Struct. Biol.* **128:** 82–97.

19. Goddard, T. D., C. C. Huang, and T. E. Ferrin. 2005. Software extensions to UCSF chimera for interactive visualization of large molecular assemblies. *Structure.* **13:** 473–482.

20. Wang, L., M. T. Walsh, and D. M. Small. 2006. Apolipoprotein B is conformationally flexible but anchored at a triolein/water interface: a possible model for lipoprotein surfaces. *Proc. Natl. Acad. Sci. USA.* **103:** 6871–6876.

21. McNamara, J. R., D. M. Small, Z. Li, and E. J. Schaefer. 1996. Differences in LDL subspecies involve alterations in lipid composition and conformational changes in apolipoprotein B. *J. Lipid Res.* **37:** 1924–1935.

22. Sandin, S., L. G. Ofverstedt, A. C. Wikstrom, O. Wrange, and U. Skoglund. 2004. Structure and flexibility of individual immunoglobulin G molecules in solution. *Structure.* **12:** 409–415.

23. Pease, R. J., R. W. Milne, W. K. Jessup, A. Law, P. Provost, J. C. Fruchart, R. T. Dean, Y. L. Marcel, and J. Scott. 1990. Use of bacterial expression cloning to localize the epitopes for a series of monoclonal antibodies against apolipoprotein B100. *J. Biol. Chem.* **265:** 553–568.

24. Young, S. G., and S. T. Hubl. 1989. An ApaLI restriction site polymorphism is associated with the MB19 polymorphism in apolipoprotein B. *J. Lipid Res.* **30:** 443–449.

25. Jiang, Z. G., D. Gantz, E. Bullitt, and C. J. McKnight. 2006. Defining lipid-interacting domains in the N-terminal region of apolipoprotein B. *Biochemistry.* **45:** 11799–11808.

26. Milne, R. W., R. Theolis, Jr., R. B. Verdery, and Y. L. Marcel. 1983. Characterization of monoclonal antibodies against human low density lipoprotein. *Arteriosclerosis.* **3:** 23–30.

27. Milne, R., R. Theolis, Jr., R. Maurice, R. J. Pease, P. K. Weech, E. Rassart, J. C. Fruchart, J. Scott, and Y. L. Marcel. 1989. The use of monoclonal antibodies to localize the low density lipoprotein receptor-binding domain of apolipoprotein B. *J. Biol. Chem.* **264:** 19754–19760.

28. Poulos, G. W. 2001. The three-dimensional structure of low-density lipoprotein via cryo-electron microscopy. [PhD dissertation]. University Microfilms International, Publication #AAT 9993754. ISBN 0-493-01861-1.

29. Yang, C. Y., Z. W. Gu, S. A. Weng, T. W. Kim, S. H. Chen, H. J. Pownall, P. M. Sharp, S. W. Liu, W. H. Li, A. M. Gotto, Jr., et al. 1989. Structure of apolipoprotein B-100 of human low density lipoproteins. *Arteriosclerosis.* **9:** 96–108.

30. Camejo, G., E. Hurt, O. Wiklund, B. Rosengren, F. Lopez, and G. Bondjers. 1991. Modifications of low-density lipoprotein induced by arterial proteoglycans and chondroitin-6-sulfate. *Biochim. Biophys. Acta.* **1096:** 253–261.

31. Mateu, L., E. M. Avila, G. Camejo, V. Leon, and N. Liscano. 1984. The structural stability of low-density lipoprotein. A kinetic X-ray scattering study of its interaction with arterial proteoglycans. *Biochim. Biophys. Acta.* **795:** 525–534.